Journal of Hazardous Materials 189 (2011) 741–748

Contents lists available at ScienceDirect

Journal of Hazardous Materials

journal homepage: www.elsevier.com/locate/jhazmat

Adsorption of Pb(II) and Cd(II) from aqueous solutions using titanate nanotubes prepared via hydrothermal method

Lin Xiong [a], Cheng Chen [a], Qing Chen [b], Jinren Ni [a,*]

[a] Department of Environmental Engineering, Peking University, The Key Laboratory of Water and Sediment Sciences, Ministry of Education, Beijing 100871, China
[b] Key Laboratory for the Physics and Chemistry of Nanodevices and Department of Electronics, Peking University, Beijing 100871, China

ARTICLE INFO

Article history:
Received 17 October 2010
Received in revised form 28 February 2011
Accepted 3 March 2011
Available online 9 March 2011

Keywords:
Titanate nanotubes
Pb(II)
Cd(II)
Kinetics
Isotherm

ABSTRACT

Titanate nanotubes (TNs) with specific surface areas of 272.31 $m^2 g^{-1}$ and pore volumes of 1.264 $cm^3 g^{-1}$ were synthesized by alkaline hydrothermal method. The TNs were investigated as adsorbents for the removal of Pb(II) and Cd(II) from aqueous solutions. The FT-IR analysis indicated that Pb(II) and Cd(II) adsorption were mainly ascribed to the hydroxyl groups in the TNs. Batch experiments were conducted by varying contact time, pH and adsorbent dosage. It was shown that the initial uptake of each metal ion was very fast in the first 5 min, and adsorption equilibrium was reached after 180 min. The adsorption of Pb(II) and Cd(II) were found to be maximum at pH in the range of 5.0–6.0. The adsorption kinetics of both metal ions followed the pseudo-second-order model. Equilibrium data were best fitted with the Langmuir isotherm model, and the maximum adsorption capacities of Pb(II) and Cd(II) were determined to be 520.83 and 238.61 mg g^{-1}, respectively. Moreover, more than 80% of Pb(II) and 85% of Cd(II) adsorbed onto TNs can be desorbed with 0.1 M HCl after 3 h. Thus, TNs were considered to be effective and promising materials for the removal of both Pb(II) and Cd(II) from wastewater.

1. Introduction

Heavy metal pollution has become a severe public health concern worldwide. Heavy metals such as lead and cadmium are persistent in nature, and can be toxic and carcinogenic. They are mainly introduced into the environment via various industrial applications [1,2]. Thus, their presence in water bodies poses harmful effects on humans and aquatic ecosystems [3]. Many technologies have been employed to eliminate heavy metal from aqueous solution, such as chemical precipitation [4], ion exchange [5], membrane separation [6] and electrolysis [7]. However, these processes have some disadvantages, including low treatment efficiency for trace amount of heavy metal ion, high operational cost and difficult further treatment due to generation of toxic sludge [8]. In contrast, adsorption could be the most cost-effective for heavy metal removal due to a variety of advantages such as easy operation, high efficiency over a wide concentration range and low secondary pollution with suitable regeneration operation [9,10]. The key to the adsorption process lies in the selection of the appropriate adsorbent. Though various substances, such as activated carbon [11], zeolite [12], clay [13], fly ash [14] and lignin [15], have been used as adsorbents in the last few years, there are still some problems in their applications, including the impurities in the adsorbents, slow adsorption kinetics, low adsorption capacities and complex regeneration [16]. Consequently, alternative materials with high sorption rate and increased capacities for heavy metals are particularly desired.

In the recent years, titanate nanotubes (TNs) prepared by hydrothermal method are of special interest. These well-defined and uniformly tubular materials are characterized by high specific surface areas and pore volumes, and they possess good ion-exchange properties [17]. Particularly, TNs have many functional hydroxyl groups. All the protons of these hydroxyl groups may be readily exchanged with heavy metal ions in aqueous solutions [18]. Moreover, the hydrothermal method is very simple with high yield and reusable alkali solutions [19]. Therefore, TNs may have great potential to adsorb heavy metals. However, so far the studies using TNs to reduce heavy metals in aqueous solutions are very limited [20]. The potential applications of adsorption onto TNs have not been explored in details. The purpose of this study is to investigate the feasibility of TNs as high efficient adsorbents for the removal of Pb(II) and Cd(II) from aqueous solutions. The effects of various operational conditions such as contact time, pH and adsorbent dosage were systematically studied. The adsorption

* Corresponding author. Tel.: +86 10 6275 1185; fax: +86 10 6275 6526.
E-mail address: nijinren@iee.pku.edu.cn (J. Ni).

0304-3894/$ – see front matter © 2011 Elsevier B.V. All rights reserved.
doi:10.1016/j.jhazmat.2011.03.006

kinetics and isotherms were also analyzed to reveal the adsorption mechanisms.

2. Materials and methods

2.1. Reagents

The reagents used in the experiments were of analytical grade and purchased from Sinopharm Chemical Reagent Co., Ltd. (Beijing, China). The stock solution (1000 mg L^{-1}) of Pb(II) or Cd(II) was prepared by dissolving stoichiometric amount of corresponding chloride ($PbCl_2$ or $CdCl_2{\cdot}2.5H_2O$) in deionized water and further diluted to the desired concentrations for the experiments.

2.2. Preparation of titanate nanotubes

The TNs were synthesized by the hydrothermal treatment of TiO_2 powder in concentrated NaOH solution as described by Chen et al. [19]. Typically, 0.3 g of TiO_2 nanoparticle powder (P25, Degussa, Germany) was added to 16.5 mL of 10 M NaOH solution. After vigorous stirring for 24 h, the mixture was autoclaved at 130 °C for 72 h. The precipitate in the autoclaved mixture was then separated by filtration and washed with deionized water until the pH value of the rinsing solution reached 7.0. Finally, the products were dried in an oven at 80 °C for 4 h.

2.3. Characterization of titanate nanotubes

Nitrogen adsorption–desorption isotherms were determined at −196 °C for Brunauer–Emmett–Teller (BET) measurements on an ASAP 2010 adsorption apparatus (Micromeritics, USA). Before adsorption, the samples were degassed at 50 °C. The BET specific surface areas were calculated in the relative pressure (P/P_0) range of 0.06–0.20. Desorption isotherms were used to determine the pore size distributions using the Barret–Joyner–Halender method. Nitrogen adsorption volumes at the relative pressure of 0.99 were used to determine the pore volumes and the average pore diameters. The point of zero charge of the sample was determined by zeta potentials in solution at different pH values in the range of 2.0–12.0. The zeta potentials were measured by a Nano-ZS90 Zetasizer (Malvern Instruments, UK). The FT-IR spectra of the samples were obtained by using a Tensor 27 FT-IR spectrometer (Bruker, Germany). All FT-IR measurements were conducted at room temperature using the KBr pellet method.

2.4. Batch adsorption test

The adsorption behaviors of Pb(II) and Cd(II) onto TNs were investigated by batch adsorption experiments on a rotary shaker at 200 rpm using 100 mL conical flasks. In a typical experiment, 10 mg of TNs was added to 50 mL heavy metal ion solution with different initial concentrations (20, 50 and 100 mg L^{-1}). The reaction temperature was kept constant at 20 ± 0.2 °C, and the solution pH was not adjusted. After different contact time intervals, aliquots of the metal ion solution were withdrawn and centrifuged at a speed of 10,000 rpm for 5 min to obtain the supernatants. The supernatants were then kept to determine the Pb(II) and Cd(II) concentrations using an inductively coupled plasma spectrometer (ICP-MS X Series II, Thermo Fisher Scientific, USA). The amount of metal ion adsorbed q_t (mg g^{-1}), at time t (min), was calculated by

$$q_t = \frac{(C_i - C_t)V}{m} \tag{1}$$

where C_i and C_t (mg L^{-1}) are initial and equilibrium concentrations of metal ion, respectively, V (L) is the volume of metal ion solution, and m (g) is the mass of the TNs.

Effect of pH on the adsorption capacity of metal ion was evaluated by agitating 100 mg L^{-1} metal ion solution with 10 mg of TNs for predetermined equilibrium time at pH ranging from 2.0 to 6.0. The pH of metal ion solution was adjusted by using 0.5 M HCl or 0.5 M NaOH. Similarly, the effect of adsorbent dosage (0.05, 0.1, 0.2 and 0.4 g L^{-1}) was also studied in batch experiments. To evaluate the capacities of TNs to remove Pb(II) and Cd(II), batch equilibrium experiments were performed with fixed adsorbent dosage of 0.2 g L^{-1} at various initial concentrations (20–200 mg L^{-1}). The amount of metal ion adsorbed at equilibrium q_e (mg g^{-1}), and the metal ion removal efficiency R (%), were computed by Eqs. (2) and (3), respectively.

$$q_e = \frac{(C_i - C_e)V}{m} \tag{2}$$

$$R = \frac{C_i - C_e}{C_i} \times 100 \tag{3}$$

where C_e (mg L^{-1}) is the equilibrium concentration of metal ion.

2.5. Adsorption kinetics modeling

To understand the adsorption mechanisms of Pb(II) and Cd(II) onto TNs, the uptake rate of both metal ions at initial concentration of 20, 50 and 100 mg L^{-1} were analyzed respectively by three kinetic models, i.e., pseudo-first-order kinetic, pseudo-second-order kinetic and intraparticle diffusion models.

The pseudo-first-order kinetic model is expressed in the following linearized form [21]

$$\log(q_e - q_t) = \log q_e - \frac{k_1}{2.303}t \tag{4}$$

where q_e and q_t (mg g^{-1}) are the amounts of metal ion adsorbed at equilibrium and elapsed time t, respectively, t (min) is contact time, and k_1 (min^{-1}) is pseudo-first-order rate constant. k_1 and q_e can be computed from the slope and intercept of the plot of $\log(q_e - q_t)$ versus t.

The pseudo-second-order kinetic model is described by the equation [22]

$$\frac{t}{q_t} = \frac{1}{k_2 q_e^2} + \frac{1}{q_e}t \tag{5}$$

where k_2 (g mg^{-1} min^{-1}) is pseudo-second-order rate constant. The values of k_2 and q_e can be calculated from the slope and intercept of the plot of t/q_t versus t.

The initial adsorption rate h (mg g^{-1} min^{-1}), is estimated at $t \to 0$ as follows

$$h = k_2 q_e^2 \tag{6}$$

The intraparticle diffusion model is used to determine the rate-limiting step if there is the possibility of intraparticle diffusion involved in the adsorption process. The equation for this model is from [23]

$$q_t = k_{int} t^{0.5} + C \tag{7}$$

where k_{int} (mg g^{-1} $min^{-0.5}$) is intraparticle diffusion rate constant, and C (mg g^{-1}) is the constant proportional to the extent of boundary layer thickness. k_{int} and C can be obtained from the plot of q_t versus $t^{0.5}$.

2.6. Adsorption isotherm modeling

The adsorption isotherm provides much information, such as the distribution of the adsorbate between the adsorbent and liquid phase, and the adsorption capacity of the adsorbent, which are

essential in design of the adsorption system. Hence, the equilibrium data were subject to simulate with three isotherm models, i.e., Langmuir, Freundlich and Temkin isotherm models.

The Langmuir model assumes that monolayer surface adsorption occurs on specific homogeneous sites and no interaction exists between the adsorbed pollutants [24]. The equation for this model can be written as follows

$$\frac{C_e}{q_e} = \frac{1}{bQ} + \frac{1}{Q}C_e \quad (8)$$

where C_e (mg L^{-1}) is the equilibrium metal ion concentration, q_e (mg g^{-1}) is the amount of metal ion adsorbed at equilibrium, Q (mg g^{-1}) is the maximum adsorption capacity of the adsorbent, and b (L mg^{-1}) is the Langmuir constant related to the free energy of adsorption. By plotting C_e/q_e versus C_e, then the slope and intercept of the linear plot can be used to determine the values of Q and b.

Based on the essential characteristic of the Langmuir model, an adsorption system can be evaluated as "favorable" or "unfavorable" in terms of a dimensionless constant, the separation factor R_L, as defined by [25]

$$R_L = \frac{1}{1 + bC_0} \quad (9)$$

where C_0 (mg L^{-1}) is initial concentration of metal ion. According to the values of R_L, the adsorption process may be classified as irreversible ($R_L = 0$), favorable ($0 < R_L < 1$), linear ($R_L = 1$) and unfavorable ($R_L > 1$).

The Freundlich isotherm is an empirical equation describing heterogeneous surface adsorption [26]. The linear form of the equation is usually expressed as

$$\log q_e = \log K_F + \frac{1}{n} \log C_e \quad (10)$$

where K_F (mg g^{-1}) is the Freundlich constant related to the adsorption capacity of the adsorbent, and n is the heterogeneity factor indicating the adsorption intensity of the adsorbent. Both constants are obtained from the slope and intercept of the linear plot of $\log q_e$ versus $\log C_e$.

The Temkin model is different from the above-mentioned isotherm models in that it considers the effect of the interaction between the adsorbed adsorbates [27]. This isotherm model is represented as follows

$$q_e = \frac{RT}{B} \ln A + \frac{RT}{B} \ln C_e \quad (11)$$

where A (L g^{-1}) and B (J mol^{-1}) are Temkin constants, R (J mol^{-1} K^{-1}) is the ideal gas constant, and T (K) is the absolute temperature. A plot of q_e versus $\ln C_e$ is used to calculate the values of A and B.

2.7. Desorption experiments

For desorption studies, 10 mg of TNs was initially contacted with 50 mL of 100 mg L^{-1} metal ion solution. After equilibrium adsorption, the equilibrium concentration (C_e) of metal ion was measured. Then the pH of the equilibrium solution was adjusted to the range of 1.0–6.0 using 0.5 M HCl or 0.5 M NaOH. Afterwards, the solution was shaken for predetermined equilibrium time. Finally, the equilibrium concentration after desorption (C_d) was measured. The percentage of desorption D (%), was calculated by

$$D = \frac{C_d - C_e}{C_i - C_e} \times 100 \quad (12)$$

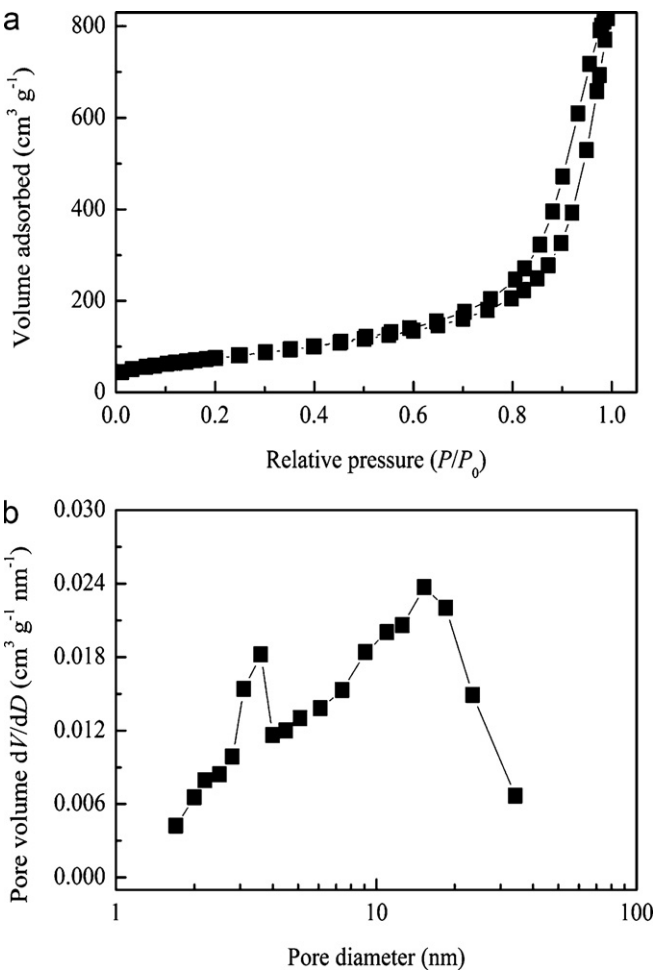

Fig. 1. (a) Nitrogen adsorption–desorption isotherms and (b) pore size distributions of the TNs.

3. Results and discussion

3.1. Characterization of TNs

The nitrogen adsorption–desorption isotherms and pore size distributions of the TNs were shown in Fig. 1(a) and (b). According to the adsorption data, Table 1 presents the surface properties of TNs. The BET specific surface areas and the single point total pore volumes were 272.31 m^2 g^{-1} and 1.264 cm^3 g^{-1}, which were much higher than that of TiO_2 (P25) by a factor of 5.8 and 7.0, respectively [28]. The obvious increase in surface areas and porosity of TNs could be ascribed to their unique morphology. Both the external and internal sides of the nanotubes contributed to the surfaces. The pores along the lengths and the interlay cavities in the walls were also accessible, in favor of the increase of the pore volumes. On the other hand, it can be observed from Fig. 1(a) that the TNs showed type IV isotherms with evident adsorption hysteresis loops in terms of BDDT classification [29], suggesting the presence of mesopores (2–50 nm). The mean pore diameter of the samples was

Table 1
Basic structure parameters of TNs.

Parameters	Values
Specific surface area (m^2 g^{-1})	272.31
Single point total pore volume (cm^3 g^{-1})	1.264
Average pore diameter (nm)	18.6
Point of zero charge	2.57

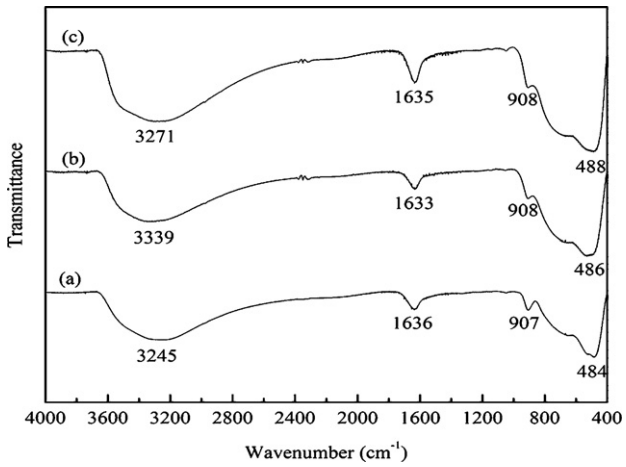

Fig. 2. The FT-IR spectra of (a) pure TNs, (b) Pb(II) loaded TNs, and (c) Cd(II) loaded TNs (resolution = 4 cm^{-1}, C_i = 100 mg/L).

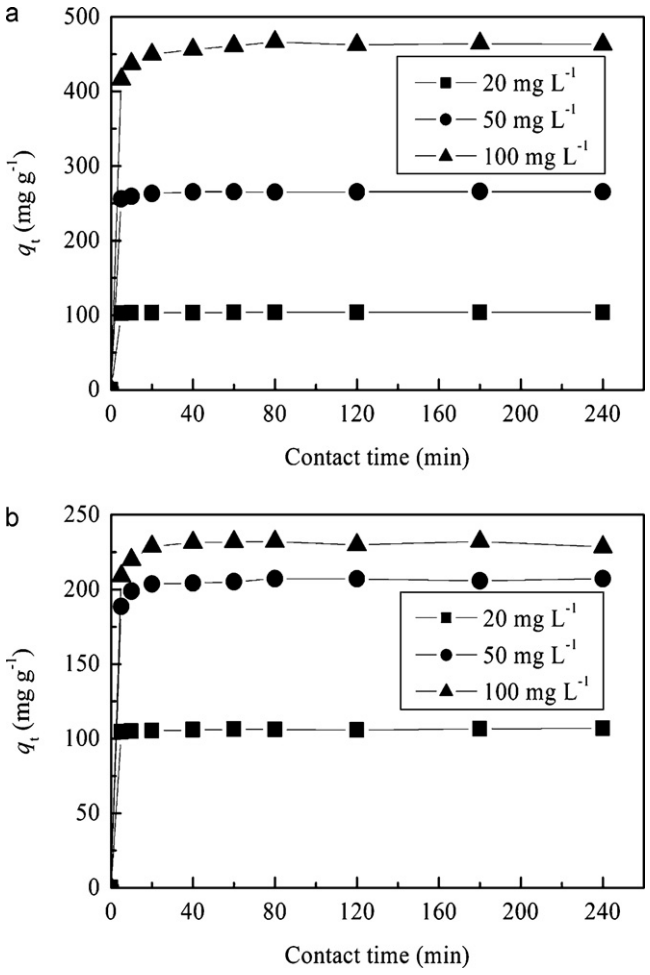

Fig. 3. Effect of contact time on adsorption of (a) Pb(II) and (b) Cd(II) by TNs at different initial concentrations (adsorbent dosage = 0.2 g L^{-1}, temperature = 20 °C and pH not adjusted).

18.6 nm (Table 1). The pore sizes exhibited bimodal distributions as shown in Fig. 1(b), i.e., smaller pores with peak diameter in the range of 3.0–4.0 nm and larger pores with peak diameter in the range of 10.0–20.0 nm. The former might correspond to the pores inside the nanotubes, and the latter were due to the voids in the aggregation of the nanotubes [30]. Because the TNs possessed large surface areas, they may expectedly provide abundant active sites and make it possible to adsorb the target contaminant molecules onto the surfaces. On the other hand, high pore volumes and mesoporous structures of the TNs allowed the fast diffusion into the pores of the contaminants. All these characteristics resulted in the improvement of adsorption capacities of TNs in gaseous or liquid adsorption. Additionally, the point of zero charge of the TN was observed at pH 2.57 (Table 1), which was much lower than that of P25 (pH 6.5, as reported in the previous study [31]). Then the surface charges of TNs would become negative when the solution pH was above the point of zero charge, which was accordingly favorable for the adsorption of cation such as Pb(II) and Cd(II).

3.2. Adsorption mechanism of metal ions onto TNs

The FT-IR spectra of TNs and metal ions loaded TNs are shown in Fig. 2. In the case of pure TNs, the spectrum (Fig. 2(a)) exhibited the absorption bands at 3245, 1636, 907 and 484 cm^{-1}. According to Chen et al. [17] and Sun et al. [32], the TNs might be constructed from trititanate ($Na_xH_{2-x}Ti_3O_7$, x = 0 or 0.75, depending on remaining sodium ions), which was composed of corrugated ribbons of edge-sharing [TiO_6] octahedrons as negatively charged layers and H^+ and Na^+ located between the layers. Then the strong absorption bands in the region of 3500–3000 cm^{-1} and the band at 1636 cm^{-1} could be attributed to the O–H stretching vibration and H–O–H binding vibration, respectively, indicating the presence of hydroxyl groups and water molecules in the TNs. The band at 907 cm^{-1} might be related to a four-coordinate Ti–O stretching vibration [32]. The band at 484 cm^{-1} was assigned to the vibration of [TiO_6] octahedron [20]. After adsorption of Pb(II) and Cd(II) by TNs, the bands at 907 and 484 cm^{-1} were just slightly shifted within the resolution range (Fig. 2(b) and (c)), revealing that both Ti–O bond and [TiO_6] octahedron had no positive effect on the adsorption of Pb(II) and Cd(II). However, it can be apparently seen that the bands of hydroxyl groups in pure TNs were significantly shifted from 3245 to 3339 cm^{-1} in Pb(II) loaded TNs and to 3271 cm^{-1} in Cd(II) loaded TNs, as shown in Fig. 2(b) and (c). This indicated that the adsorption could have mainly occurred through the interaction between metal ions and hydroxyl groups of the TNs. Furthermore, considering the model for the formation of trititanate nanotubes proposed by Zhang et al. [33], the negative charges of the [TiO_6] layers might be compensated by H^+ or Na^+ on the inner and outer surfaces of the tubes. Then it was believed that H^+ ions from hydroxyl groups or Na^+ ions could be exchanged with metal ions in the adsorption process, and the adsorbed metal ions might bond with O atoms after the adsorption. Hence it was speculated that ion exchange and oxygen bonding might be the principal mechanisms for the adsorption of Pb(II) and Cd(II). These mechanisms were in agreement with that for Pd(II) adsorption over titanate nanotubes suggested by Kochkar et al. [34]. Similar complex mechanisms were also proposed by Chen et al. [20] for the adsorption of Pb(II) onto titanate nanotubes made by microwave hydrothermal method.

3.3. Adsorption studies

3.3.1. Effect of contact time

The effect of contact time on the adsorption of Pb(II) and Cd(II) were investigated to determine the time taken for adsorption equilibrium. The results were illustrated in Fig. 3. It was evident that adsorption capacities of Pb(II) and Cd(II) increased sharply within the first 20 min of contact for different initial concentrations of 20, 50 and 100 mg L^{-1}. With the further increase of contact time, the adsorption of Pb(II) and Cd(II) gave a slow approach towards equilibrium until 180 min. Afterwards, no appreciable changes in terms of the amount of adsorption were noticed. Therefore, 180 min

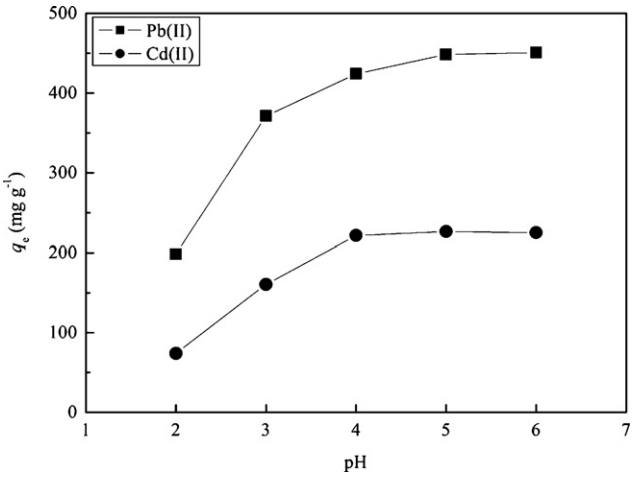

Fig. 4. Effect of pH on adsorption of Pb(II) and Cd(II) by TNs (adsorbent dosage = 0.2 g L^{-1}, initial metal ion concentration = 100 mg L^{-1}, temperature = 20 °C and contact time = 180 min).

of contact time was considered to be appropriate for equilibrium adsorption of Pb(II) and Cd(II) in all subsequent experiments. It was also observed that the uptake of Pb(II) and Cd(II) were very rapid in the first 5 min, which were probably attributed to a number of available active adsorption sites onto TNs [9]. As contact time increased, the adsorption sites gradually became exhausted. Later the uptake rate was decreased on account of the slow pore diffusion of metal ions into the bulk of TNs. The measured data could be further used for the evaluation of the adsorption kinetics of Pb(II) and Cd(II).

3.3.2. *Effect of pH*

The pH of the solution is recognized as an important parameter that significantly affects adsorption of metal ions. For this reason, the effect of pH on adsorption of Pb(II) and Cd(II) were studied. As shown in Fig. 4, the pH of the solution was varied from 2.0 to 6.0, which was appropriate to prevent precipitation of metals in the form of hydroxides under higher pH conditions. Both Pb(II) and Cd(II) adsorbed onto TNs experienced similar rapid rise at initial pH of 2.0–4.0, followed by a slow increase of Pb(II) at pH 4.0–5.0 to an approximately constant at pH 5.0–6.0, and a less significant change of Cd(II) at pH 4.0–6.0. The optimum adsorption capacities of Pb(II) and Cd(II) were found in the pH range of 5.0–6.0.

The effect of pH on adsorption of both metal ions could be reasonably explained by the net charges on the surface of TNs and H^+ ions competition for adsorption sites [35,36]. Because the resulting point of zero charge was found to be at pH 2.57, the overall charges on the adsorbent surfaces were positive at pH 2.0 and H^+ ions would strongly compete for available active sites with metal cations, resulting in the low uptake of metal ions (198.45 and 74.10 mg g^{-1} for Pb(II) and Cd(II), respectively). As the pH increased (3.0–5.0), the surfaces of TNs became negatively charged and the negative charges also increased, which enhanced the adsorption of positively charged Pb(II) and Cd(II) by electrostatic attraction. In the meanwhile, the concentration of H^+ ions decreased with the increase of pH, and fewer H^+ ions were available to compete with metal ions for adsorption sites. At higher pH (5.0–6.0), the concentration of H^+ ions was far lower than that of metal ions, so most adsorption sites were occupied by metal ions and the competition of trace amounts of H^+ ions might be negligible. That was why the adsorption of metal ions changed very little in the pH range of 5.0–6.0. Similar trend were observed for the adsorption of Pb(II) and Cd(II) onto other materials such as bael leaves [8], saw dust [37] and activated alumina [3]. Additionally, since the natural pH of Pb(II) and Cd(II) were just within this optimum pH range, the pH of the solution was not adjusted in further experiments.

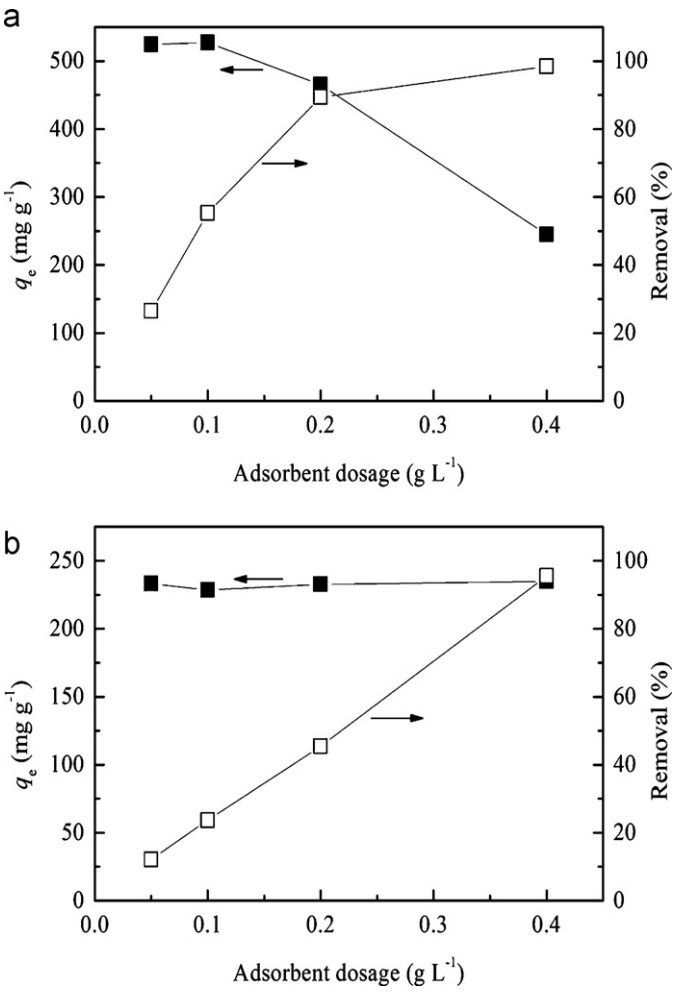

Fig. 5. Effect of adsorbent dosage on adsorption of (a) Pb(II) and (b) Cd(II) by TNs (initial metal ion concentration = 100 mg L^{-1}, temperature = 20 °C, contact time = 180 min and pH not adjusted).

3.3.3. *Effect of adsorbent dosage*

The effect of adsorbent dosage on the adsorption capacities and percentage removal of Pb(II) and Cd(II) by TNs are depicted in Fig. 5. For Pb(II), it can be seen that the adsorption capacity at equilibrium kept nearly constant at low adsorbent dosage (0.05–0.1 g L^{-1}) and decreased sharply as the dosage increased from 0.1 to 0.4 g L^{-1} (Fig. 5(a)). As to Cd(II), there was no significant change in adsorption capacity in the whole dosage range (Fig. 5(b)). On the other hand, when the dosage of TNs increased from 0.05 to 0.4 g L^{-1}, the removal of Pb(II) increased from 26.5% to 98.4%, and Cd(II) increased from 12.1% to 95.5%, respectively, suggesting that both Pb(II) and Cd(II) could be highly removed when the adsorbent dosage reached 0.4 g L^{-1}. The results may be explained by adsorption surface area and available adsorption sites [38]. At low adsorbent dosage, i.e., no more than 0.1 g L^{-1}, the adsorption sites were saturated through the uptake of Pb(II), resulting in saturated Pb(II) adsorption. However, with a higher adsorbent dosage (0.1–0.4 g L^{-1}), the adsorption sites would be excessive for the adsorption reaction, which led to the unsaturation of adsorption sites. Additionally, higher dosage might cause the aggregation of the adsorbents. Such aggregation could reduce the surface areas of the adsorbents [10]. As a result, the amount adsorbed per unit mass of adsorbent decreased. In contrast, the adsorption surface became saturated with Cd(II) in the whole

Table 2
Kinetic parameters for the adsorption of Pb(II) and Cd(II) by TNs at 20 °C.

Kinetic models	Parameters	Initial Pb(II) concentration (mg L^{-1})			Initial Cd(II) concentration (mg L^{-1})		
		20	50	100	20	50	100
Pseudo-first-order kinetic model	$q_{e,cal}$[a] (mg g^{-1})	6.61	32.85	106.80	9.24	34.30	55.72
	k_1 (min^{-1})	0.0838	0.0783	0.0648	0.0626	0.0784	0.1001
	R^2	0.6078	0.6987	0.7643	0.5308	0.7382	0.8827
Pseudo-second-order kinetic model	$q_{e,cal}$[a] (mg g^{-1})	103.82	266.60	465.55	106.37	206.57	234.41
	k_2 (g mg^{-1} min^{-1})	0.1134	0.0155	0.0032	0.0640	0.0122	0.0073
	h (mg g^{-1} min^{-1})	1222.522	1101.635	697.890	724.156	518.876	402.775
	R^2	1.0000	1.0000	1.0000	1.0000	1.0000	1.0000
Intraparticle diffusion model	k_{int} (mg g^{-1} min$^{-0.5}$)	0.1709	1.6930	7.3559	0.3164	2.1906	5.2615
	C (mg g^{-1})	102.42	253.70	408.82	103.82	189.31	201.03
	R^2	0.9616	0.8727	0.8561	0.9748	0.7212	0.8524
	$q_{e,mea}$[b] (mg g^{-1})	103.81	266.09	464.37	106.57	205.75	232.19

[a] The calculated adsorption capacity at equilibrium, namely q_e in Eqs. (4), (5) and (6), respectively.
[b] The measured adsorption capacity at equilibrium.

adsorbent dosage range of 0.05–0.4 g L^{-1}, making the adsorption capacity of Cd(II) nearly constant. However, the increase of the adsorbent dosage resulted in the increase of adsorption surface areas and active sites on the adsorbents, so it resulted in the increment of adsorption removal of both metal ions. These observations in the present study were in agreement with those reported by Gupta et al. [16] for hexavalent chromium adsorption using carbon slurry.

3.4. Adsorption kinetics

The parameters of three kinetic models are calculated and listed in Table 2. The pseudo-first-order model showed poor fitting to the experimental data with very low correlation coefficients, i.e., ranging from 0.6078 to 0.7643 for Pb(II) and from 0.5308 to 0.8827 for Cd(II), respectively. The calculated equilibrium adsorption capacities ($q_{e,cal}$) deviated too much from the measured values ($q_{e,mea}$). This suggested that the pseudo-first-order model failed to describe the adsorption process correctly. The fitting of experimental data to the intraparticle diffusion model was also not satisfactory. The correlation coefficient values for this model were relatively poor, though they were better than those of the pseudo-first-order model. Furthermore, the linear plots of q_t versus $t^{0.5}$ did not pass through the origin since the values of C were not equal to zero. So it might be implied that the intraparticle diffusion was not the rate-limiting step in the metal ion adsorption process [23]. In contrast, the pseudo-second-order model provided excellent correlation coefficients ($R^2 > 0.9999$) and achieved good agreement between $q_{e,cal}$ and $q_{e,mea}$ of Pb(II) and Cd(II). Hence it can be concluded that the adsorption of Pb(II) and Cd(II) onto TNs perfectly obeyed the pseudo-second-order kinetic model, indicating that the rate-controlling step might be chemisorptions [22]. Similar kinetics were observed in the adsorption of Pb(II) onto steel slag [39] and Cd(II) onto loess soil [40]. Moreover, with the increase of initial concentrations from 20 to 100 mg L^{-1}, there were gradual decrease in the rate constants (k_2) and the initial adsorption rate (h) for both metal ions. This indicated that faster uptake of each metal ion onto TNs would be obtained at lower initial concentration.

3.5. Adsorption isotherms

Table 3 lists the constants and correlation coefficients involved in the three isotherm models. It was found that the Langmuir model exhibited good fit to the adsorption data for Pb(II) and Cd(II) with extremely high correlation coefficients ($R^2 = 0.9997$, 0.9996). The correlation coefficients of the Temkin model were 0.7180 for Pb(II) and 0.8028 for Cd(II), indicating the data did not show satisfactory compliance with this model. In contrast, the Freundlich model represented the poor fit to the data for both metal ions since the correlation coefficients were much lower than those of other two models. The fact that the adsorption isotherms of Pb(II) and Cd(II) exhibited good Langmuir behaviors implied that the existence of homogeneous active sites within the TNs and the monolayer adsorption of Pb(II) and Cd(II) onto the adsorbent. Moreover, the dimensionless constant R_L ranged from 0.004 to 0.041 for Pb(II) and from 0.006 to 0.053 for Cd(II), so the adsorption for both metal ions by TNs can be considered to be favorable. Also, the monolayer maximum adsorption capacities were calculated as 520.83 and 238.61 mg g^{-1} for Pb(II) and Cd(II), respectively. Compared with several alternative adsorbents in the literature presented in Table 4, it was apparent that TNs in this study had much higher adsorption capacities for both metal ions than other materials, indicating the TNs were promising adsorption materials for the effective removal of Pb(II) and Cd(II) from aqueous solutions.

3.6. Desorption studies

To evaluate the regeneration performance of the TNs, desorption experiments were conducted with TNs that had fully adsorbed 100 mg L^{-1} Pb(II) and Cd(II) by altering the pH in the range of 1.0–6.0. As shown in Fig. 6, the desorption percentage were up to 82.3% and 88.1% respectively for Pb(II) and Cd(II) at pH 1.0 (0.1 mol/L HCl) after 3 h. With increasing pH as it was less than 5.0, the desorp-

Table 3
Isotherm constants for the adsorption of Pb(II) and Cd(II) by TNs at 20 °C.

Adsorption isotherm models	Isotherm constants	Metal ions	
		Pb(II)	Cd(II)
Langmuir isotherm model	Q (mg g^{-1})	520.83	238.61
	b (L mg^{-1})	1.088	0.814
	R^2	0.9997	0.9996
Freundlich isotherm model	K_F (mg g^{-1})	247.10	154.68
	n	5.386	10.491
	R^2	0.5667	0.7239
Temkin isotherm model	A (L g^{-1})	135.501	1.719×10^4
	B (J mol^{-1})	42.183	147.357
	R^2	0.7180	0.8028

Table 4
Comparison of monolayer maximum capacities of some adsorbents for Pb(II) and Cd(II) from aqueous solutions.

Adsorbents	Adsorbates	Monolayer maximum capacities ($mg\,g^{-1}$)	References
Activated carbon	Pb(II)	43.85	[41]
Manganese oxide coated zeolite	Pb(II)	60.09	[42]
Montmorillonite–illite type of clay	Pb(II)	52.00	[43]
Manganese oxide-coated carbon nanotubes	Pb(II)	78.74	[44]
Titanate nanotubes	Pb(II)	520.83	This study
Activated carbon	Cd(II)	19.50	[45]
Loess soil	Cd(II)	9.37	[40]
Beidellite	Cd(II)	42.01	[46]
Multiwalled carbon nanotubes	Cd(II)	10.86	[47]
Titanate nanotubes	Cd(II)	238.61	This study

tion percentage of both metal ions decreased. When the solution pH further increased (5.0–6.0), the desorption capacities were almost negligible. Similar results were also reported on the adsorption and desorption of Pb(II) ions onto bael leaves [8]. The mechanism of desorption might be attributed to the replacement of H^+ ions on the metal loaded adsorbents [17]. With the decrease of pH, there was an increase in H^+ ion concentration. The abundant H^+ ions in the solution would compete with the metal ions for the exchange sites. As H^+ ions occupied the sites in the adorbents, the adsorbed metal ions were released into the aqueous solution. The aforementioned results confirmed the possibility of fast recovery of the TNs by reducing pH, which should be of significance to practical applications.

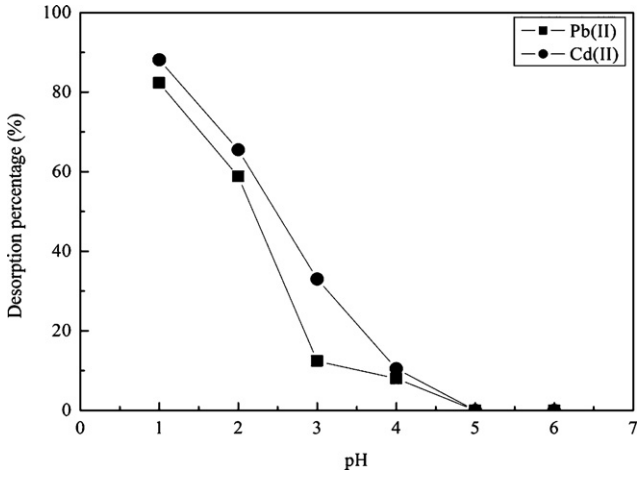

Fig. 6. Effect of pH on desorption efficiency of Pb(II) and Cd(II) onto TNs (adsorbent dosage = 0.2 g L^{-1}, initial metal ion concentration = 100 mg L^{-1} and temperature = 20 °C).

4. Conclusions

Titanate nanotubes were prepared by hydrothermal method. Their possible applications for the removal of heavy metals were investigated. Particular attention was paid to the utilization of TNs as novel effective adsorbents for the removal of Pb(II) and Cd(II) from aqueous solutions. The analyses of nitrogen adsorption–desorption isotherms showed that the mesoporous TNs exhibited larger specific surface areas of 272.31 $m^2\,g^{-1}$ and higher pore volumes of 1.264 $cm^3\,g^{-1}$. Furthermore, FT-IR spectra revealed that the hydroxyl groups in the TNs were responsible for Pb(II) and Cd(II) adsorption. Batch adsorption tests demonstrated that the adsorption was affected by various conditions such as contact time, solution pH and adsorbent dosage. The adsorption rate of each metal ion was very fast in the first 5 min, and the adsorption equilibrium was achieved after 180 min. The maximum amounts of Pb(II) and Cd(II) adsorbed were detected in the pH range of 5.0–6.0, in which the natural pH values of Pb(II) and Cd(II) lie. The kinetic studies indicated that the adsorption of Pb(II) and Cd(II) onto TNs best fit the pseudo-second-order kinetic model. The study on equilibrium adsorption revealed that the Langmuir model was most appropriate to describe Pb(II) and Cd(II) adsorption behaviors. The monolayer maximum adsorption capacities of Pb(II) and Cd(II) were found to be 520.83 and 238.61 mg g^{-1}, respectively. The adsorption–desorption results showed that the TNs could be readily regenerated after adsorption using 0.1 M HCl. Therefore, the TNs exhibited great potential for the removal of Pb(II) and Cd(II) from wastewater in engineering practices.

Acknowledgements

Financial support is from National Major Special Program of Science and Technology on Water Pollution Control and Treatment (Grant No. 2009ZX07212-001). The authors would like to acknowledge the two anonymous reviewers for their constructive comments and suggestions.

References

[1] B.L. Martins, C.C.V. Cruz, A.S. Luna, C.A. Henriques, Sorption and desorption of Pb^{2+} ions by dead *Sargassum* sp. biomass, Biochem. Eng. J. 27 (2006) 310–314.
[2] M. Mohapatra, S. Anand, Studies on sorption of Cd(II) on Tata chromite mine overburden, J. Hazard. Mater. 148 (2007) 553–559.
[3] T.K. Naiya, A.K. Bhattacharya, S.K. Das, Adsorption of Cd(II) and Pb(II) from aqueous solutions on activated alumina, J. Colloid Interface Sci. 333 (2009) 14–26.
[4] G. Macchi, D. Marani, M. Pagano, G. Bagnuolo, A bench study on lead removal from battery manufacturing wastewater by carbonate precipitation, Water Res. 30 (1996) 3032–3036.
[5] A. Dabrowski, Z. Hubicki, P. Podkoscielny, E. Robens, Selective removal of the heavy metal ions from waters and industrial wastewaters by ion-exchange method, Chemosphere 56 (2004) 91–106.
[6] H.R. Mortaheb, A. Zolfaghari, B. Mokhtarani, M.H. Amini, V. Mandanipour, Study on removal of cadmium by hybrid liquid membrane process, J. Hazard. Mater. 177 (2010) 660–667.
[7] S. Chellammal, S. Raghu, P. Kalaiselvi, G. Subramanian, Electrolytic recovery of dilute copper from a mixed industrial effluent of high strength COD, J. Hazard. Mater. 180 (2010) 91–97.
[8] S. Chakravarty, A. Mohanty, T.N. Sudha, A.K. Upadhyay, J. Konar, J.K. Sircar, A. Madhukar, K.K. Gupta, Removal of Pb(II) ions from aqueous solution by adsorption using bael leaves (*Aegle marmelos*), J. Hazard. Mater. 173 (2010) 502–509.
[9] M. Rafatullah, O. Sulaiman, R. Hashim, A. Ahmad, Adsorption of copper (II), chromium (III), nickel (II) and lead (II) ions from aqueous solutions by meranti sawdust, J. Hazard. Mater. 170 (2009) 969–977.
[10] L. Semerjian, Equilibrium and kinetics of cadmium adsorption from aqueous solutions using untreated *Pinus halepensis* sawdust, J. Hazard. Mater. 173 (2010) 236–242.
[11] Z.R. Yue, S.E. Bender, J.W. Wang, J. Economy, Removal of chromium Cr(VI) by low-cost chemically activated carbon materials from water, J. Hazard. Mater. 166 (2009) 74–78.
[12] A.M. El-Kamash, A.A. Zaki, M.A. El Geleel, Modeling batch kinetics and thermodynamics of zinc and cadmium ions removal from waste solutions using synthetic zeolite A, J. Hazard. Mater. 127 (2005) 211–220.

[13] S. Veli, B. Alyuz, Adsorption of copper and zinc from aqueous solutions by using natural clay, J. Hazard. Mater. 149 (2007) 226–233.
[14] V.C. Srivastava, I.D. Mall, I.M. Mishra, Modelling individual and competitive adsorption of cadmium(II) and zinc(II) metal ions from aqueous solution onto bagasse fly ash, Sep. Sci. Technol. 41 (2006) 2685–2710.
[15] D. Mohan, C.U. Pittman, P.H. Steele, Single, binary and multi-component adsorption of copper and cadmium from aqueous solutions on Kraft lignin—a biosorbent, J. Colloid Interface Sci. 297 (2006) 489–504.
[16] V.K. Gupta, A. Rastogi, A. Nayak, Adsorption studies on the removal of hexavalent chromium from aqueous solution using a low cost fertilizer industry waste material, J. Colloid Interface Sci. 342 (2010) 135–141.
[17] Q. Chen, L.M. Peng, Structure and applications of titanate and related nanostructures, Int. J. Nanotechnol. 4 (2007) 44–65.
[18] D.V. Bavykin, J.M. Friedrich, F.C. Walsh, Protonated titanates and TiO_2 nanostructured materials: synthesis, properties, and applications, Adv. Mater. 18 (2006) 2807–2824.
[19] Q. Chen, W.Z. Zhou, G.H. Du, L.M. Peng, Trititanate nanotubes made via a single alkali treatment, Adv. Mater. 14 (2002), 1208-+.
[20] Y.C. Chen, S.L. Lo, J. Kuo, Pb(II) adsorption capacity and behavior of titanate nanotubes made by microwave hydrothermal method, Colloids Surf., A 361 (2010) 126–131.
[21] S. Lagergren, Zur theorie der sogenannten adsorption gelöster stoffe, K. Sven. Vetenskapsakad. Handl. 24 (1898) 1–39.
[22] Y.S. Ho, G. McKay, Sorption of dye from aqueous solution by peat, Chem. Eng. J. 70 (1998) 115–124.
[23] W.J. Weber, J.C. Morris, Kinetics of adsorption on carbon from solution, J. Sanit. Eng. Div. Am. Soc. Civ. Eng. 89 (1963) 31–59.
[24] I. Langmuir, The adsorption of gases on plane surfaces of glass, mica and platinum, J. Am. Chem. Soc. 40 (1918) 1361–1403.
[25] K.R. Hall, L.C. Eagleton, A. Acrivos, T. Vermeule, Pore- and solid-diffusion kinetics in fixed-bed adsorption under constant-pattern conditions, Ind. Eng. Chem. Fund. 5 (1966) 212–223.
[26] H. Freundlich, Über die adsorption in lösungen, Z. Phys. Chem. 57 (1906) 385–470.
[27] M.J. Temkin, V. Pyzhev, Recent modifications to Langmuir isotherms, Acta Physicochim. USSR 12 (1940) 217–222.
[28] L. Xiong, Y. Yang, J.X. Mai, W.L. Sun, C.Y. Zhang, D.P. Wei, Q. Chen, J.R. Ni, Adsorption behavior of methylene blue onto titanate nanotubes, Chem. Eng. J. 156 (2010) 313–320.
[29] S. Brunauer, L.S. Deming, W.E. Deming, E. Teller, On a theory of the van der Waals adsorption of gases, J. Am. Chem. Soc. 62 (1940) 1723–1732.
[30] J.G. Yu, J.C. Yu, M.K.P. Leung, W.K. Ho, B. Cheng, X.J. Zhao, J.C. Zhao, Effects of acidic and basic hydrolysis catalysts on the photocatalytic activity and microstructures of bimodal mesoporous titania, J. Catal. 217 (2003) 69–78.
[31] H. Park, W. Choi, Effects of TiO_2 surface fluorination on photocatalytic reactions and photoelectrochemical behaviors, J. Phys. Chem. B 108 (2004) 4086–4093.
[32] X.M. Sun, Y.D. Li, Synthesis and characterization of ion-exchangeable titanate nanotubes, Chem. Eur. J. 9 (2003) 2229–2238.
[33] S. Zhang, L.M. Peng, Q. Chen, G.H. Du, G. Dawson, W.Z. Zhou, Formation mechanism of $H_2Ti_3O_7$ nanotubes, Phys. Rev. Lett. 91 (2003) 256103.
[34] H. Kochkar, A. Turki, L. Bergaoui, G. Berhault, A. Ghorbel, Study of Pd(II) adsorption over titanate nanotubes of different diameters, J. Colloid Interface Sci. 331 (2009) 27–31.
[35] H. Aydin, Y. Buluta, C. Yerlikaya, Removal of copper (II) from aqueous solution by adsorption onto low-cost adsorbents, J. Environ. Manage. 87 (2008) 37–45.
[36] S. Liang, X.G. Guo, N.C. Feng, Q.H. Tian, Adsorption of Cu^{2+} and Cd^{2+} from aqueous solution by mercapto-acetic acid modified orange peel, Colloids Surf., B 73 (2009) 10–14.
[37] S.Q. Memon, N. Memon, S.W. Shah, M.Y. Khuhawar, M.I. Bhanger, Sawdust—a green and economical sorbent for the removal of cadmium (II) ions, J. Hazard. Mater. 139 (2007) 116–121.
[38] K. Jayaram, I.Y.L.N. Murthy, H. Lalhruaitluanga, M.N.V. Prasad, Biosorption of lead from aqueous solution by seed powder of *Strychnos potatorum* L., Colloids Surf., B 71 (2009) 248–254.
[39] S.Y. Liu, J. Gao, Y.J. Yang, Y.C. Yang, Z.X. Ye, Adsorption intrinsic kinetics and isotherms of lead ions on steel slag, J. Hazard. Mater. 173 (2010) 558–562.
[40] Y. Wang, X.W. Tang, Y.M. Chen, L.T. Zhan, Z.Z. Li, Q. Tang, Adsorption behavior and mechanism of Cd(II) on loess soil from China, J. Hazard. Mater. 172 (2009) 30–37.
[41] J. Acharya, J.N. Sahu, C.R. Mohanty, B.C. Meikap, Removal of lead(II) from wastewater by activated carbon developed from tamarind wood by zinc chloride activation, Chem. Eng. J. 149 (2009) 249–262.
[42] W.H. Zou, R.P. Han, Z.Z. Chen, J. Shi, H.M. Liu, Characterization and properties of manganese oxide coated zeolite as adsorbent for removal of copper(II) and lead(II) ions from solution, J. Chem. Eng. Data 51 (2006) 534–541.
[43] J.U.K. Oubagaranadin, Z.V.P. Murthy, Adsorption of divalent lead on a montmorillonite–illite type of clay, Ind. Eng. Chem. Res. 48 (2009) 10627–10636.
[44] S.G. Wang, W.X. Gong, X.W. Liu, Y.W. Yao, B.Y. Gao, Q.Y. Yue, Removal of lead(II) from aqueous solution by adsorption onto manganese oxide-coated carbon nanotubes, Sep. Purif. Technol. 58 (2007) 17–23.
[45] M.M. Rao, A. Ramesh, G.P.C. Rao, K. Seshaiah, Removal of copper and cadmium from the aqueous solutions by activated carbon derived from *Ceiba pentandra* hulls, J. Hazard. Mater. 129 (2006) 123–129.
[46] O. Etci, N. Bektas, M.S. Oncel, Single and binary adsorption of lead and cadmium ions from aqueous solution using the clay mineral beidellite, Environ. Earth Sci. 61 (2010) 231–240.
[47] Y.H. Li, J. Ding, Z.K. Luan, Z.C. Di, Y.F. Zhu, C.L. Xu, D.H. Wu, B.Q. Wei, Competitive adsorption of Pb^{2+}, Cu^{2+} and Cd^{2+} ions from aqueous solutions by multiwalled carbon nanotubes, Carbon 41 (2003) 2787–2792.